



Complexation of silver(I) cation by a series of heterosubstituted dipyridyl ligands

Nathan L. Brennan^a, Charles L. Barnes^b, Eric Bosch^{a,*}

^a Chemistry Department, Missouri State University, Springfield, MO 65897, USA

^b Chemistry Department, University of Missouri, Columbia, MO 65211, USA

ARTICLE INFO

Article history:

Received 3 June 2010

Received in revised form 22 July 2010

Accepted 27 July 2010

Available online 3 August 2010

Keywords:

Silver complexes

Bipyridyl ligands

X-ray crystal structures

ABSTRACT

The synthesis of a series of dipyridyl ligands based on 1,2-bis(2'-pyridylethynyl)benzene and their complexation of silver cation is described. NMR binding studies confirm that the incorporation of thioether appendages results in an increased binding constant while ether appendages result in similar or lower binding constants as compared to the unsubstituted ligand. X-ray crystallographic analysis confirms that steric hindrance is critical.

© 2010 Elsevier B.V. All rights reserved.

1. Introduction

We earlier reported the design and synthesis of a simple *trans* coordinating ligand, 1,2-bis(2'-pyridylethynyl) benzene (**1** in Scheme 1A), that was particularly well suited for the coordination of silver(I) and palladium(II) cation [1,2]. We modeled the planar conformation of the ligand as shown in Scheme 1 and noted that this conformation would position the pyridyl N-atoms in the ideal position at 4.3 Å apart to coordinate transition metal cations like silver(I) that favor linear coordination geometry [3]. Note that the pyridyl–pyridyl distance in simple linear 2:1 pyridine–silver complexes is approximately 4.26 Å for the perchlorate, tetrafluoroborate and hexafluorophosphate salts [4]. Indeed, we reported the formation and the X-ray structural characterization of the essentially planar coordination complexes of the ligand with silver(I) and palladium(II) cations (Scheme 1B). In this paper we report our results with a series of modified ligands with heteroatom-containing side-arms that we envisioned would wrap around the bound metal cation and possible even assist in the initial binding process. These ligands are shown in Scheme 1C.

2. Experimental

2.1. Synthesis

2.1.1. Synthesis of **2**

Diethynyl benzene (0.126 g, 1 mmol), 2-bromo-5-hydroxymethyl pyridine [5] (0.419 g, 2.25 mmol), triphenylphosphine

(15 mg, 0.057 mmol), and diethylamine (15 mL) were added to a 50 mL round bottom flask under an argon atmosphere. Argon was bubbled through the mixture for 10 min. Copper iodide (4 mg, 0.02 mmol), and dichloro bis(triphenylphosphine)palladium(II) (15 mg, 0.02 mmol) were added and the solution warmed to 80 °C under an argon atmosphere. After 96 h TLC indicated that the reaction was complete. The crude reaction mixture was purified using flash chromatography with ethyl acetate as eluant. Complex **2** was recrystallized from dichloromethane as light yellow crystals (62% yield). M.p.: 149–154 °C. ¹H NMR (400 MHz, DMSO d-6) δ 7.89 (t, *J* = 8 Hz, 2H), 7.74 (dd, *J* = 3.2, 6.0 Hz, 2H), 7.71 (d, *J* = 8.4 Hz, 2H), 7.54 (dd, *J* = 3.2, 6.0 Hz, 2H), 7.53 (d, *J* = 7.2 Hz, 2H), 5.53 (t, *J* = 5.6 Hz, 2H), 4.61 (d, *J* = 6.0 Hz, 4H); ¹³C NMR (100 MHz, DMSO d-6) δ 163.5, 141.7, 137.9, 132.8, 130.3, 126.5, 125.2, 121.0, 94.0, 87.2, 64.72.

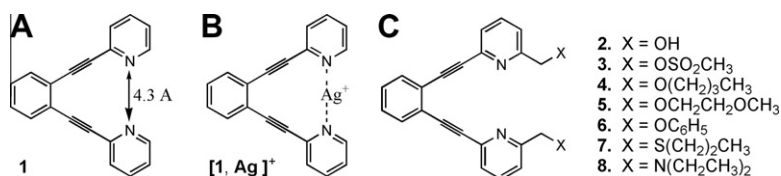
2.1.2. Synthesis of dimesylate **3**

Diol **2** (1 mmol, 0.340 g), triethylamine (3.0 mmol, 0.42 mL) and THF (15 mL) were added to a dry 25 mL round bottom flask under an argon atmosphere. The mixture was cooled in an ice bath and methylsulfonyl chloride (3.0 mmol, 0.232 mL) added. After the reaction was complete saturated aqueous sodium bicarbonate was added to the reaction mixture which was then extracted using dichloromethane. The dichloromethane solution was washed with a saturated brine solution and then dried over magnesium sulfate and the solvent removed yielding **3** as off-white fluffy crystals in almost quantitative yield. M.p.: 149–150 °C. ¹H NMR (400 MHz, CDCl₃) δ 7.80 (t, *J* = 7.6 Hz, 2H), 7.69 (d, *J* = 8.4 Hz, 2H), 7.66 (dd, *J* = 3.2, 6.0 Hz, 2H), 7.47 (d, *J* = 8.0 Hz, 2H), 7.40 (dd, *J* = 3.2 Hz, 6.0 Hz, 2H), 5.36 (s, 4H), 3.10 (s, 6H); ¹³C NMR (100 MHz, CDCl₃) δ 154.3, 143.2, 137.5, 132.3, 129.1, 127.6, 125.2, 121.6, 92.3, 88.4, 71.1, 38.2.

* Corresponding author. Address: 901 South National Avenue, Springfield, MO 65897, USA. Tel.: +1 417 836 4277; fax: +1 417 836 5507.

E-mail address: ericbosch@missouristate.edu (E. Bosch).

URL: <http://chemistry.missouristate.edu/31072.htm> (E. Bosch).



Scheme 1.

2.1.3. Synthesis of **4**

Sodium hydride (60% in mineral oil, 0.2 mmol, 0.008 mg) and THF (15 mL) were placed in a dry 25 mL round bottom flask under an argon atmosphere. Butanol (0.25 mmol, 0.023 mL) was added and the resultant mixture stirred for 30 min under argon. The solution was then cooled in an ice bath and the dimesylate **3** (0.1 mmol, 50 mg) added as a solid. After 30 min the reaction mixture was allowed to warm to room temperature and stirred for 7 h when TLC indicated that the reaction was complete. Saturated aqueous ammonium chloride and ethyl acetate were added to the solution. The organic layer was separated, washed with water and brine and dried over anhydrous sodium sulfate. The solvent was removed under vacuum and the product isolated by flash chromatography using a 1:4 mixture of ethyl acetate and hexane as eluant yielding the product as a yellow oil in 60% yield. ^1H NMR (400 MHz, DMSO *d*-6) δ 7.90 (t, J = 3.6 Hz, 2H), 7.735 (m, 4H), 7.55 (dd, J = 3.2 Hz, 6.0 Hz, 2H), 7.48 (d, J = 7.6 Hz, 2H), 4.57 (s, 4H), 3.52 (t, J = 6.4 Hz, 4H), 1.56 (quintet, J = 1.6 Hz, 4H), 1.35 (sextet, J = 7.2 Hz, 4H), 0.89 (t, J = 7.2 Hz, 6H); ^{13}C NMR (100 MHz, CDCl_3) δ 159.7, 142.5, 136.6, 132.1, 128.6, 126.2, 125.5, 120.3, 92.9, 87.7, 73.5, 71.0, 31.8, 19.3, 13.9.

2.1.4. Synthesis of **5**

Sodium hydride (60% in mineral oil, 0.2 mmol, 0.008 mg) and THF (5 mL) were placed in a dry 25 mL round bottom flask under an argon atmosphere. The mixture was cooled to 0 °C and methoxyethanol (0.25 mmol, 0.02 mL) added. The solution was stirred for 30 min under argon and then a separate solution of the dimesylate **3** (0.1 mmol, 50 mg) in THF (10 mL) was then added dropwise. The reaction mixture was allowed to warm to room temperature and stirred until TLC indicated that the reaction was complete. Following the usual workup **5** was obtained as a clear yellow oil in near quantitative yield. ^1H NMR (400 MHz, CDCl_3) δ 7.697 (t, J = 7.6 Hz, 2H), 7.649 (dd, J = 3.2, 6.0 Hz, 2H), 7.609 (d, J = 7.6 Hz, 2H), 7.490 (d, J = 8.0 Hz, 2H), 7.359 (dd, J = 3.2, 6.0 Hz, 2H), 4.742 (s, 4H), 3.740 (m, 4H), 3.624 (m, 4H), 3.419 (s, 6H). ^{13}C NMR (400 MHz, CDCl_3) δ 159.5, 142.8, 137.0, 132.4, 129.0, 126.6, 125.7, 120.7, 93.1, 87.9, 74.2, 72.1, 70.4, 59.3.

2.1.5. Synthesis of **6**

Sodium hydride (60% in mineral oil, 0.2 mmol, 0.008 mg) and THF (5 mL) were placed in a dry 25 mL round bottom flask under an argon atmosphere. The mixture was cooled to 0 °C and phenol (0.2 mmol, 0.019 mg) was then added and the solution stirred for 30 min. A solution of the dimesylate **3** (0.1 mmol, 50 mg) in THF (10 mL) was then added dropwise. The resultant mixture was brought to 40 °C and stirred under argon until TLC indicated that the reaction was complete. The usual workup yielded **6** as white fluffy crystals in near quantitative yield. M.p.: 123–126 °C. ^1H NMR (400 MHz, DMSO *d*-6) δ 7.888 (t, J = 7.6 Hz, 2H), 7.782 (d, J = 8.0 Hz, 2H), 7.769 (dd, J = 3.2 Hz, 6.0 Hz, 2H), 7.545 (d, J = 8.0 Hz, 2H), 7.559 (dd, J = 3.2, 6.0 Hz, 2H), 7.303 (t, J = 7.6 Hz, 4H), 7.027 (d, J = 8.8 Hz, 4H), 6.962 (t, J = 6.8 Hz, 2H), 5.217 (s, 4H). ^{13}C NMR (400 MHz, DMSO *d*-6) δ 157.9, 157.6, 141.7, 137.6, 132.1, 129.7, 129.5, 126.6, 124.2, 121.5, 120.9, 114.6, 92.9, 86.9, 69.7.

2.1.6. Synthesis of **7**

Sodium hydride (0.008 mg, 60% in mineral oil, 0.2 mmol) and THF (15 mL) were placed in a dry 25 mL round bottom flask under an argon atmosphere. The sodium hydride solution was cooled to –15 °C before butanethiol (0.2 mmol, 0.021 mL) was added. The resultant solution was stirred 15 min before dimesylate **3** (0.1 mmol, 50 mg) was then added as a solid. TLC analysis indicated that the reaction was complete after 40 min at –15 °C. The usual workup yielded **7** in low yield as an orange oil. ^1H NMR (400 MHz, DMSO *d*-6) δ 7.848 (t, J = 7.6 Hz, 2H), 7.744 (dd, J = 3.2, 6.0 Hz, 2H), 7.695 (d, J = 6.8, 2H), 7.545 (dd, J = 3.2, 6.0 Hz, 2H), 7.481 (d, J = 7.6 Hz, 2H), 3.848 (s, 4H), 2.472 (t, J = 7.2 Hz, 4H), 1.464 (quintet, J = 7.6 Hz, 4H), 1.291 (sextet, J = 7.2 Hz, 4H), 0.812 (t, J = 7.2 Hz, 6H). ^{13}C NMR (400 MHz, DMSO *d*-6) δ 160.2, 141.8, 137.8, 132.6, 130.1, 126.3, 124.8, 123.6, 93.7, 87.0, 37.4, 31.3, 31.0, 21.7, 13.9.

2.1.7. Synthesis of **8**

A solution of the dimesylate **3** (0.2 g, 0.4 mmol) in acetonitrile (40 mL) was prepared in a dry round bottom flask under an argon atmosphere. Diisopropylethylamine (0.4 mL, 2.5 mmol) and diethylamine (0.17 mL, 1.6 mmol) were added and the resultant mixture was heated to 45 °C. After the reaction was complete it was diluted with dichloromethane and washed with water and dried over sodium sulfate. The solvent was evaporated and the product purified by flash chromatography using methanol as eluant to yield **8** as a dark brown gel. ^1H NMR (400 MHz, DMSO *d*-6) δ 7.882 (t, J = 7.6 Hz, 2H), 7.738 (dd, J = 3.6, 6.0 Hz, 2H), 7.373 (d, J = 7.6 Hz, 2H), 7.530 (m, 4H), 3.681 (s, 4H), 2.510 (q, J = 7.2 Hz, 8H), 0.985 (t, J = 6.8 Hz, 12H). ^{13}C NMR (400 MHz, CDCl_3) δ 161.6, 142.3, 136.3, 132.1, 128.5, 125.8, 125.6, 122.0, 93.2, 87.4, 59.7, 47.5, 12.0.

2.1.8. Formation of complex **[2, Ag]⁺ CF₃SO₃⁻**

A solution of silver(I) trifluoromethane sulfonate (10.3 mg, 0.04 mmol) and **2** (11.2 mg, 0.04 mmol) was prepared in warm nitromethane (2 mL). This was cooled to room temperature and carefully layered over dichloromethane (3 mL) in a screw-cap vial. The vial was sealed and allowed to stand in the dark. Clear block-shaped crystals formed after 24 h. The solution was removed and the crystals dried in the atmosphere.

2.1.9. Formation of complex **[6, Ag]⁺ CF₃SO₃⁻**

A solution of silver(I) trifluoromethane sulfonate (10.3 mg, 0.04 mmol) and **6** (15.8 mg, 0.04 mmol) was prepared in warm dichloromethane (3 mL). The vial was sealed and allowed to stand in the dark. Clear plate-like crystals formed.

2.2. Binding constants

We titrated each of the ligands with silver(I) triflate and used ^1H NMR to monitor changes in the chemical shifts to determine binding constants. All titrations were performed by stepwise addition of silver(I) triflate into a solution of the ligand. The titrations were continued until there was no further change in chemical shift indicating that there was no “free”, or uncomplexed, ligand. Plots of the change in chemical shift against the ratio of added silver(I) con-

firmed the formation of 1:1 complexes. The initial and final chemical shifts were then used to determine the relative concentrations of free ligand, complexed ligand and free and complexed silver(I) in solution. An initial titration experiment was usually run to obtain approximate values of the formation constant along with estimates of the reliability of the results using the “*p*” value as defined by Weber [6]. The concentrations of ligand and silver(I) to be used in the experiment were then modified to ensure that valid reliable results were obtained with the next titration experiment.

The initial ligand concentration was in the range of 0.5–8.8 mM (2, 8.0; 4, 8.8; 5, 8.5; 6, 8.2; 7, 0.5 and 8, 8.0 mM). For each experiment a stock solution of the silver(I) triflate was prepared in DMSO d-6 (140–212 mM) and titrated into the solution of the ligand in DMSO d-6 in aliquots of between 5 and 50 μ L. In a few instances where the “endpoint” of the titration was unclear the final concentration of silver salt was increased by addition of a small portion of the solid salt. In all cases the solutions and NMR samples were mixed using a vortex genie to ensure homogeneous samples before measurement of the NMR spectra. All ^1H NMR spectra were recorded using 32 scans. The resulting concentration and chemical shift data was entered into an Excel worksheet and calculations were performed in Excel. A similar titration was performed with the unsubstituted ligand, 1,2-bis(2'-pyridylethynyl)benzene, compound 1 (see Scheme 1) as reference.

2.3. X-ray structure determinations

Crystals were mounted on small cryoloops using viscous hydrocarbon oil. Data were collected using a Bruker Apex2 CCD diffractometer equipped with Mo K α radiation with $\lambda = 0.71073$ Å. Data collection at low temperatures was facilitated by use of a Kryoflex system with an accuracy of ± 1 K. Initial data processing was carried

out using the Apex II softwaresuite [7]. Structures were solved by direct methods using SHELXS-97 and refined using standard alternating least-squares cycles against F^2 using SHELXL-97 [8]. The program X-Seed was used as a graphical interface [9]. Methine and methylene hydrogen atoms attached to carbon were placed in idealised positions and refined with a riding model. Methyl hydrogen atoms attached to carbon were positioned according to maximum electron density. Hydrogen atoms attached to oxygen were placed in idealised positions based on maximum electron density. For complex [2, Ag] $^+$ OTf $^-$ the highest residual electron density peak appeared close to C22 suggesting disorder between the two hydroxymethyl sidearms. For complex [6, Ag] $^+$ OTf $^-$ the triflate was disordered over two positions and it was modeled using a free variable, which converged to 0.89, as well as bond distance and bond angle restraints. The oxygen and fluorine were allowed to remain isotropic during refinement since they tended to become non-positive definite when refined anisotropically. The highest two residual electron density peaks were centered around the disordered triflate suggesting that there may be other less populated positions for the triflate. The crystallographic data for these structures is collected in Table 1.

3. Results and discussion

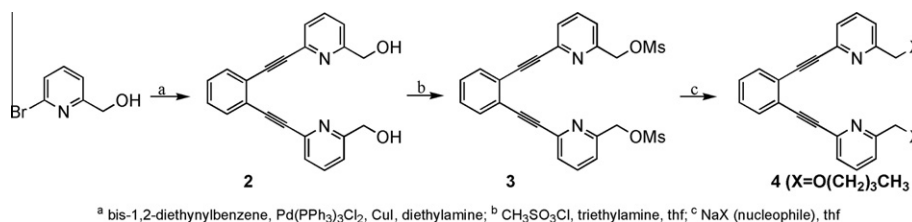
3.1. Synthesis

The synthetic strategy that we used to synthesize compounds 2–8 is shown specifically for compound 4 in Scheme 2.

The synthetic route began with the preparation of 2-bromo-6-hydroxymethylpyridine from 2,6-dibromopyridine using the procedure developed by Verhoeven et al. [5]. This bromopyridine was then coupled with 1,2-diethynylbenzene to yield the dihy-

Table 1
Crystal data and structure refinement for compound 2, [2, Ag] $^+$ OTf $^-$ and [6, Ag] $^+$ OTf $^-$.

Compound	2	[2, Ag] $^+$ OTf $^-$	[6, Ag] $^+$ OTf $^-$
Empirical formula	C ₂₂ H ₁₆ N ₂ O ₂	C ₂₃ H ₁₆ AgF ₃ N ₂ O ₅ S	C ₃₅ H ₂₄ AgF ₃ N ₂ O ₅ S
Formula weight	340.37	597.31	749.49
Color, habit	colorless, block	colorless, block	colorless, block
Temperature (K)	173(2)	173(2)	173(2)
Wavelength (Å), source	0.71073 Mo K α	0.71073 Mo K α	0.71073 Mo K α
Crystal system, space group	monoclinic, $P2_1/c$	triclinic, $P\bar{1}$	monoclinic, $P12_1/c_1$
Unit cell dimensions			
<i>a</i> (Å)	13.258(3)	7.4221(7)	18.2234(13)
<i>b</i> (Å)	7.6640(15)	12.4394(12)	9.6662(7)
<i>c</i> (Å)	17.501(4)	13.7826(13)	19.1686(14)
α (°)	90	114.6540(10)	90
β (°)	108.49(3)	96.553(2)	114.5620(10)
γ (°)	90	97.641(2)	90
Volume (Å ³)	1686.5(6)	1125.73(19)	3071.0(4)
<i>Z</i> , <i>D</i> _{calc} (mg/m ³)	4, 1.341	2, 1.762	4, 1.621
Absorption coefficient (mm ⁻¹)	0.087	1.052	0.79
<i>F</i> (0 0 0)	712	596	1512
Crystal size (mm)	0.15 × 0.25 × 0.30	0.30 × 0.15 × 0.05	0.19 × 0.44 × 0.54
θ Range for data collection (°)	2.45–25.00	1.66–27.15	1.23–27.14
Limiting indices	–15 ≤ <i>h</i> ≤ 15, –9 ≤ <i>k</i> ≤ 9, –20 ≤ <i>l</i> ≤ 20	–9 ≤ <i>h</i> ≤ 9, –15 ≤ <i>k</i> ≤ 15, –17 ≤ <i>l</i> ≤ 15	–23 ≤ <i>h</i> ≤ 23, –12 ≤ <i>k</i> ≤ 12, –24 ≤ <i>l</i> ≤ 24
Reflections collected/unique	17297/2966 [<i>R</i> _{int} = 0.0265]	8020/4852 [<i>R</i> _{int} = 0.0245]	37674/6794 [<i>R</i> _{int} = 0.0245]
Completeness (θ) (% , °)	100, 25.0	97.0, 27.15	99.8, 27.14
Absorption correction	multi-scan	semi-empirical	numerical
Maximum and minimum transmission	0.98 and 0.89	0.95 and 0.74	0.87 and 0.69
Refinement method	Full-matrix least-squares on F^2	Full-matrix least-squares on F^2	Full-matrix least-squares on F^2
Data/restraints/parameters	2966/0/237	4852/0/320	6794/12/467
Goodness-of-fit on F^2	1.039	1.053	1.035
Final <i>R</i> indices [<i>I</i> > 2 σ (<i>I</i>)]	<i>R</i> ₁ = 0.0306, <i>wR</i> ₂ = 0.0775	<i>R</i> ₁ = 0.0433, <i>wR</i> ₂ = 0.1125	<i>R</i> ₁ = 0.0242, <i>wR</i> ₂ = 0.0618
<i>R</i> indices (all data)	<i>R</i> ₁ = 0.0370, <i>wR</i> ₂ = 0.0839	<i>R</i> ₁ = 0.0591, <i>wR</i> ₂ = 0.1227	<i>R</i> ₁ = 0.0289, <i>wR</i> ₂ = 0.0653
Largest difference in peak and hole (e Å ⁻³)	0.17 and –0.18	1.86 and –0.73	0.55 and –0.40



Scheme 2.

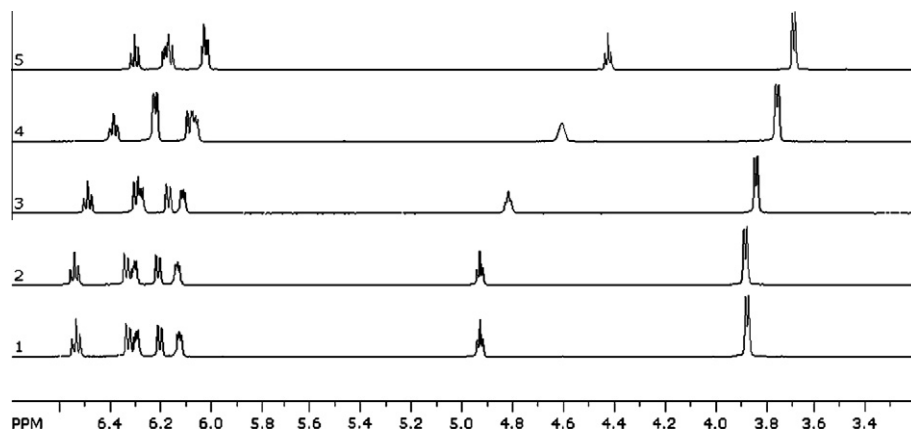
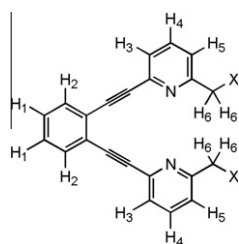


Fig. 1. Series of ¹H NMR spectra obtained on titration of ligand **2** with silver(I) triflate in dimethylsulfoxide-d₆. The top spectrum, (5), corresponds to **2** alone (no silver ion present). The ratio of silver(I):**2** for each of the other spectra is: 0.5 in (4); 1.0 in (3); 2.0 in (2); and 3.0 in (1).

droxy ligand **2** in moderate yield. Compound **2** was then transformed into the corresponding dimesylate **3** using methanesulfonylchloride and triethylamine in tetrahydrofuran solvent. Further transformation of the dimesylate by reaction with a series of nucleophiles, prepared by reaction of the corresponding alcohol or thiol with sodium hydride, yielded the desired ligands **4–8**. Thus, for example, reaction of **3** with sodium butoxide yielded the diether **4** in moderate yield. Reaction of the dimesylate **3** with diethylamine in the presence of diisopropylethylamine and acetonitrile yielded the diamine **8**.

3.2. Binding constants

There were several things to verify with the binding experiments. Most notably, we needed to establish that a 1:1 complex was formed and that all the ligands indeed bound silver as a linear 1:1 complex as shown in Scheme 1B. Ideally we were hoping to clearly evaluate the involvement of the side arm in the binding process. A representative titration experiment, the titration of dihydroxy ligand **2** with silver(I) triflate, is shown in Fig. 1. In this plot the aromatic, methylene and hydroxyl protons shift downfield however it is noteworthy that there is no change in chemical shift between spectra 2 and 1 indicating that the ligand was totally bound to silver.



Scheme 3.

For clarity and consistency in the subsequent discussion the hydrogen atoms were assigned and numbered according to the diagram in Scheme 3.

In order to confirm that a 1:1 complex was formed the change in chemical shift of each of the protons was plotted against the molar ratio of ligand:silver. A typical plot is shown in Fig. 2 for proton H-4. The fitted lines confirm that a 1:1 complex is indeed formed. It is noteworthy that a similar plot was obtained for unsubstituted ligand **1** as well as the other substituted ligands.

The chemical shift changes were collected for each of the ligands and are collated in Table 2. It is important to note that they are similar in magnitude and direction to those obtained in a titration using the unsubstituted ligand 1,2-bis(2'-pyridylethynyl)benzene **1**.

This confirms that similar linear 1:1 complexes as shown in Scheme 1B were obtained with the sidearm substituted ligands and the unsubstituted ligand. There are slight differences for thioether **7** which will be discussed later. The titrations for ligands **2** and **4–7** were performed at concentrations that were chosen to give ratios of the concentration of complex to the maximum possible concentration of complex between 0.2 and 0.8 – this is called

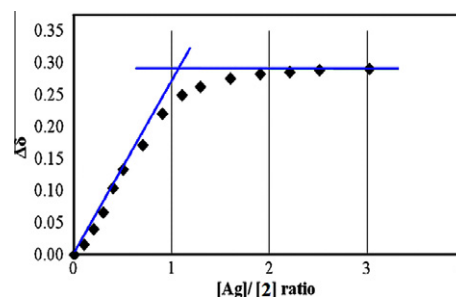


Fig. 2. Plot of change in chemical shift of H₄ against the ratio of silver(I) cation to ligand **2**.

Table 2
Total chemical shift change (ppm) of each proton in ligands **1**, **2** and **4–7**.

Ligand	H ₁	H ₂	H ₃	H ₄	H ₅	H ₆
1	0.105	0.123	0.207	0.216	0.305	–
2	0.120	0.143	0.207	0.29	0.227	0.232
4	0.128	0.147	0.236	0.309	0.293	0.281
5	0.128	0.146	0.236	0.262	0.279	0.295
6	0.123	0.144	0.221	0.332	0.299	0.292
7	0.086	0.084	0.300	0.247	0.243	0.387

the “*p*-value” [6]. In our studies most *p*-values were in the range of 0.4–0.76. For each of the ligands the formation constant was individually calculated for each of the protons listed in Table 1 and then averaged. It is noteworthy that the values were consistent throughout. The formation constants are presented in Table 3.

Surprisingly the hydroxymethyl substituent had no noticeable effect on the binding of silver cation while the addition of the ether substituents generally lowered the binding constant with the lowest binding constant at $1.8 \times 10^2 \text{ M}^{-1}$ for the diphenylether **6**. Improved binding and the highest binding constant was observed for the dithioether **7** with $K = 7.8 \times 10^3 \text{ M}^{-1}$. The diamine ligand **8** gave anomalous results and will not be further discussed here.

These results can be put into context by comparing these binding constants to binding constants reported for other 1:1 polypyridyl:silver(I) complexes in DMSO solution. Thus, the ligands **2** and **7** have higher binding constants than the bidentate ligand 2,2'-bipyridine and the tridentate ligand 2,2',6',2''-terpyridine which have log *K* values of 2.08 and 3.03, respectively. The binding is, however, significantly weaker than that of the flexible tridentate ligand bis((2-pyridyl)methyl)amine with log *K* = 4.37.[10]

3.3. X-ray analyses

The X-ray structure of ligand **2** was first obtained followed by the structures of the silver complexes [2, Ag]⁺ OTf[−] and [6, Ag]⁺ OTf[−]. The structure of **2** in Fig. 3A shows the planar conformation of the ligand with only one of the nitrogen atoms of the two pyridine rings facing towards the metal binding site. This is reasonable due to electronic repulsion of the pyridyl N non bonding electron pairs. Interestingly only one of the two hydroxyl groups is involved

Table 4
Selected bond lengths (Å) and angles (°) for complexes [2, Ag]⁺ OTf[−] and [6, Ag]⁺ OTf[−].

	Complex [2, Ag] ⁺ OTf [−]	Complex [6, Ag] ⁺ OTf [−]
<i>Bond lengths</i>		
Ag(1)–N(1)	2.203(3)	2.163 (1)
Ag(1)–N(2)	2.181(3)	2.169 (1)
Ag(1)–O(1)	2.570(4)	2.404(1) ^a
<i>Bond angles</i>		
N(2)–Ag(1)–N(1)	177.19(11)	165.34(5)
N(1)–Ag(1)–O(1)	68.80(11)	–

^a Interaction with the triflate anion.

in hydrogen bonding, O(2)–H···N(1), which establishes one-dimensional hydrogen-bonded chains of the ligand within the crystals.

The X-ray structure of two silver complexes were obtained and these help understand the results. In Fig. 3B, the structure of the silver(I) complex with ligand **2** it is apparent that in the crystalline solid only one hydroxyl oxygen interacts with the silver cation. While it is reasonable to conclude that this is also a function of crystal packing which would favor a planar conformation and therefore restrict the side arm interaction to one side it is also quite likely that in solution there is a dynamic interaction between both hydroxyl groups and the metal center. This latter proposal is supported by the observation that the hydroxyl protons shift downfield by 0.64 ppm on complexation with silver(I). The structure of the complex between the phenylether **6** and silver(I) triflate shown in Fig. 3C shows no interaction between the ether oxygen atoms and the silver cation. In this case the conformation is unlikely to be influenced significantly by crystal packing since one phenyl ring is not coplanar with the rest of the complex. Instead there is a weak interaction with the triflate anion, shown as a dashed line in Fig. 3C, which is unlikely to persist in DMSO solution. It is more reasonable to assume that the large phenyl rings hinder the binding and do not allow for interaction with the ether oxygen atoms. In both these complexes the N–Ag bond lengths are typical for pyridine–silver complexes ranging from 2.163 to 2.203 Å (see Table 4) [4]. The N–Ag–N bond angle is essentially linear in unhindered complex [2, Ag]⁺ OTf[−] at 177.19° while the bond angle is significantly distorted in the more hindered complex [6, Ag]⁺ OTf[−] at 165.34°.

Table 3
Binding of silver cation by ligands **1**, **2** and **4–7**.

Ligand	1	2	4	5	6	7
Formation constant (M ^{−1})	1.3×10^3	1.3×10^3	7.0×10^2	6.6×10^2	1.8×10^2	7.8×10^3
Log <i>K</i>	3.11	3.11	2.85	2.82	2.26	3.89

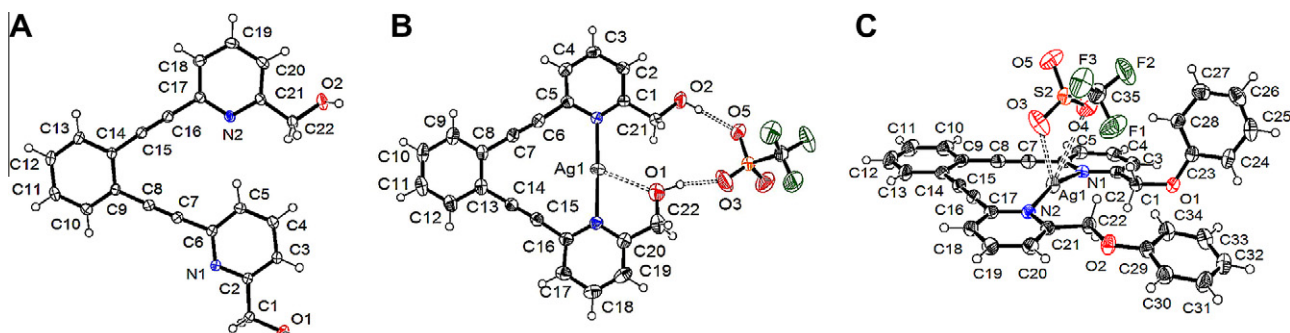


Fig. 3. (A) View of the asymmetric unit of the X-ray crystal structure of compound **2**. (B) View of complex [2, Ag]⁺ OTf[−] crystallized from nitromethane solution. (C) Oblique view of complex [6, Ag]⁺ OTf[−] crystallized from dichloromethane solution. All displacement ellipsoids drawn at the 50% level.

4. Conclusions

It is reasonable to conclude that oxygen-containing sidearms have minimal effect on silver(I) binding except for the very hindered ethers which have a slightly negative effect on binding by the ligands. Thus the binding constant for ligands **1** and **2** were essentially the same – despite the involvement of the alcohol oxygen as evidenced both by the large downfield shift of the OH and methylene protons shown in Fig. 1 and the clear Ag–O interaction shown in the X-ray crystal structure. The steric effect of the larger ether sidearm apparently is more pronounced than any cooperative oxygen–silver coordination leading to decreased binding constants. This was most noticeable with the phenylether ligand **6**. This ligand has a binding constant almost one order of magnitude lower than unsubstituted ligand **1**. Indeed the crystal structure shown in Fig. 3C shows no interaction between the ether O atoms and the silver cation. In contrast the thioether derivative displayed 60% stronger binding so the sulfur atom is clearly involved. This is presumably a result of the stronger affinity of silver for sulfur due to the softer nature of the sulfur.

Acknowledgment

This research was supported by the National Science Foundation, Grant 0415711. The Missouri State University Provost Incentive Fund funded the purchase of the X-Ray diffractometer.

Appendix A. Supplementary material

Supplementary data associated with this article can be found, in the online version, at doi:10.1016/j.ica.2010.07.078.

References

- [1] (a) E. Bosch, C.L. Barnes, *Inorg. Chem.* 40 (2001) 3097;
(b) E. Bosch, C.L. Barnes, *J. Coord. Chem.* 56 (2003) 329.
- [2] See also: (a) Y.Z. Hu, C. Chamchoumis, J.S. Grebowicz, R.P. Thummel, *Inorg. Chem.* 41 (2002) 2296;
(b) E.J. Fiscus, S. Shotwell, R.C. Layland, M.D. Smith, H.-C. zur Loye, U.H.F. Bunz, *Chem. Commun.* (2001) 2674.
- [3] Calculated using Spartan '08 Windows distributed by Wavefunction, Inc., 18401 VonKarman Avenue, Suite 370, Irvine, CA 92612, USA.
- [4] C.Y. Chen, J.Y. Zeng, H.M. Lee, *Inorg. Chem. Acta* 360 (2007) 21.
- [5] D. Cai, D.L. Hughes, T.R. Verhoeven, *Tetrahedron Lett.* 37 (1996) 2537.
- [6] (a) G. Weber, in: B. Pullman, M. Weissbluth (Eds.), *Molecular Biophysics*, Academic Press, New York, 1965, pp. 369–397.;
(b) Also see discussion in: C.S. Wilcox, in: H.-J. Schneider, H. Dürr (Eds.), *Frontiers in Supramolecular Organic Chemistry and Photochemistry*, VCH, Weinheim, 1991, pp. 123–143.;
(c) H.-J. Schneider, R. Kramer, S. Simova, U. Schneider, *J. Am. Chem. Soc.* 110 (1988) 6442–6448.
- [7] ApexII Suite, Bruker AXS Ltd., Madison, WI, 2006.
- [8] G.M. Sheldrick, *Acta Crystallogr., Sect. A* 64 (2008) 112.
- [9] L.J. Barbour, *J. Supramol. Chem.* 1 (2001) 189.
- [10] S. Del Piero, R. Fedele, A. Melchior, R. Portanova, M. Tolazzi, E. Zangrando, *Inorg. Chem.* 46 (2007) 4683.